Inorg. Chem. **2002**, *41*, 1292–1298

Nanoscale Characterization of Redox and Acid Properties of Keggin-Type Heteropolyacids by Scanning Tunneling Microscopy and Tunneling Spectroscopy: Effect of Heteroatom Substitution

In K. Song,[†,‡] Russell B. Shnitser,[†] Jennifer J. Cowan,[§] Craig L. Hill,[§] and Mark A. Barteau*[,†]

Center for Catalytic Science and Technology, Department of Chemical Engineering, University of Delaware, Newark, Delaware 19716, and Department of Chemistry, Emory University, Atlanta, Georgia 30322

Received August 3, 2001

Nanoscale characterization of acid and redox properties of Keggin-type heteropolyacids (HPAs) with different heteroatoms, $H_nMW_{12}O_{40}$ (M = P, Si, B, Co), was carried out by scanning tunneling microscopy (STM) and tunneling spectroscopy (TS) in this study. HPA samples were deposited on highly oriented pyrolytic graphite surfaces to obtain images and tunneling spectra by STM before and after pyridine adsorption. All HPA samples formed well-ordered 2-dimensional arrays on graphite before and after pyridine exposure. NDR (negative differential resistance) peaks were observed in the tunneling spectra. Those measured for fresh HPA samples appeared at less negative voltages with increasing reduction potential of the HPAs and with increases in the electronegativity of the heteroatom, but with decreases in the overall negative charge of the heteropolyanions. These results support the conclusion that more reducible HPA samples show NDR behavior at less negative applied voltages in their tunneling spectra. Introduction of pyridine into the HPA arrays increased the lattice constants of the 2-dimensional HPA arrays by ca. 6 Å. Exposure to pyridine also shifted NDR peak voltages of $H_nMW_{12}O_{40}$ (M = P, Si, B, Co) samples to less negative values in the TS measurements. The NDR shifts of HPAs obtained before and after pyridine adsorption were correlated with the acid strengths of the HPAs, suggesting that tunneling spectra measured by STM could serve to probe acid properties of HPAs. These results show how one can relate the bulk acid and redox properties of HPAs to surface properties of nanostructured HPA monolayers determined by STM.

Introduction

Scanning tunneling microscopy (STM) has demonstrated the ability to image conductive surfaces as well as adsorbed molecules with angstrom-scale resolution, and has become a powerful and successful tool for surface and interface analyses.[1−4] With advances in instruments and experimental techniques, many insulating materials such as Langmuir−Blodgett films,[5] polypropylene chains,[6] aniline,[7] self-assemblies of 1-nitronaphthalene,[8] adenine,[9] tetraphenylporphyrin,[10] and disulfides[11] have been successfully imaged using STM by depositing these materials on conductive substrates such as gold and graphite. In relation to catalytic reactions, images of adsorbed molecules on catalyst surfaces such as CO on Rh(111),[12] oxygen on Pd(111),[13] benzoic acid on Cu(110),[14] and methoxy and formate species on Cu(110)[15]

* To whom correspondence should be addressed. Phone: (302) 831-8905. Fax: (302) 831-8201. E-mail: barteau@che.udel.edu.
† University of Delaware.
‡ Present address: Department of Industrial Chemistry, Kangnung National University, Kangnung 210-702, Korea.
§ Emory University.

(1) Upward, M. D.; Beton, P. H.; Moriarty, P. *Surf. Sci.* **1999**, *441*, 21.
(2) Gesquière, A.; Abdel-Mottaleb, M. M.; De Schryver, F. C. *Langmuir* **1999**, *15*, 6821.
(3) Sato, T.; Kitamura, S.-I.; Iwatsuki, M. *Surf. Sci*. **2000**, *445*, 130.
(4) Wan, L.-J.; Shundo, S.; Inukai, J.; Itaya, K. *Langmuir* **2000**, *16*, 64.
(5) Takimoto, K.; Kuroda, R.; Shindo, S.; Yasuda, S.; Matsuda, H.; Eguchi, K.; Nakagiri, T. *J. Vac. Sci. Technol., B* **1997**, *15*, 1429.
(6) Carroll, D. L.; Czerw, R.; Tekeleab, D.; Smith, D. W., Jr. *Langmuir* **2000**, *16*, 3574.
(7) Tomimoto, H.; Sumii, R.; Shitota, N.; Yagi, S.; Taniguchi, M.; Sekitani, T.; Tanaka, K. *J. Vac. Sci. Technol., B* **2000**, *18*, 2335.
(8) Böhringer, M.; Morgenstern, K.; Schneider, W.-D.; Wühn, M.; Wöll, C.; Berndt, R. *Surf. Sci*. **2000**, *444*, 199.
(9) Edelwirth, M.; Freud, J.; Sowerby, S. J.; Heckl, W. M. *Surf. Sci*. **1998**, *417*, 201.
(10) Boeckl, M. S.; Bramblett, A. L.; Hauch, K. D.; Sasaki, T.; Ratner, B. D.; Rogers, J. W., Jr. *Langmuir* **2000**, *16*, 5644.
(11) Noh, J.; Hara, M. *Langmuir* **2000**, *16*, 2045.
(12) Cernota, P.; Rider, K.; Yoon, H. A.; Salmeron, M.; Somorjai, G. A. *Surf. Sci*. **2000**, *445*, 249.
(13) Steltenpohl, A.; Memmel, N. *Surf. Sci*. **1999**, *443*, 13.

10.1021/ic010832d CCC: $22.00
Published on Web 01/30/2002

have also been successfully probed by STM. However, it can be very difficult to distinguish between different adsorbed molecules with similar sizes and structures. The difficulties may arise from rapid surface diffusion, electric field effects,[16] or the absence of molecular states near E_F. When one cannot easily distinguish between chemically inequivalent sites or adsorbates with nearly identical geometric structures and sizes, or when the STM image is of low resolution, tunneling spectroscopy (TS), based only on differences in the electronic structure of surface species, can be utilized as a valuable technique for this purpose.[17−19] For example, it was demonstrated that two types of Li clusters adsorbed on a Si(001) surface could be distinguished by their current−voltage ($I-V$) spectra.[17] TS has also proven effective in probing the redox properties of heteropolyacid monolayers.[20−23]

Heteropolyacids (HPAs), also known as polyoxometalates (POMs), are early-transition-metal oxygen anion clusters that exhibit very interesting properties depending on their molecular size, composition, and architecture.[24−26] As catalysts, they have been utilized in several commercial processes such as vapor-phase oxidation of methacrolein into methacrylic acid,[27] and have been shown to carry out a variety of acid−base and oxidation reactions in the laboratory.[28−31] Their excellent thermal stability[32] also makes HPAs good candidates for application in catalysts and sensors that may require extreme environments.

It has previously been shown by several research groups[33−35] that 2-dimensional ordered monolayer arrays of heteropoly- and isopolyacids can be formed on conductive substrates and imaged with molecular resolution by STM. In recent STM studies,[20−23,36−39] we have demonstrated that HPAs deposited on graphite surfaces form well-ordered 2-dimensional arrays and exhibit distinctive $I-V$ behavior referred to as negative differential resistance (NDR) in their tunneling spectra. The NDR phenomenon in electrically insulating overlayers has been explained in terms of resonant tunneling through a double-barrier quantum well.[40−42] Tunneling spectra exhibiting NDR features are resolved at spatially well-resolved positions in the HPA arrays corresponding to individual HPA molecules, and thus can be utilized as a direct tool to distinguish different sites in arrays of HPA mixtures.[43] We have also shown that NDR peak voltages of HPAs are closely related to the electronic properties of HPAs and, in turn, to the redox potentials of HPAs.[20−23] These can be influenced by the identity of the countercations,[20,21,23,37] framework metal cations,[21−23] and adsorbed organic molecules.[38,39] Countercations with higher electronegativities produce shifts of NDR peak voltages for heteropolyanions to less negative values. However, the dependence of NDR peak voltages on heteroatom substitution of HPAs has not previously been explored. The acid and redox properties of bulk HPAs have often been modified by replacing the protons with metal cations and/or by changing the heteroatom or the framework transition-metal atoms.[44]

In this work, nanoscale characterization of acid and redox properties of heteroatom-substituted Keggin-type[45] HPAs, $H_nMW_{12}O_{40}$ (M = P, Si, B, Co), was carried out by STM and TS. HPA samples were deposited on a highly oriented pyrolytic graphite (HOPG) surface to obtain images and tunneling spectra by STM before and after pyridine adsorption. The observed NDR peak voltages of HPA monolayers were correlated with the redox properties as well as with the acid properties of HPAs. This study shows how one can relate the bulk properties of HPAs to surface properties of nanostructured HPA monolayers determined by STM.

Experimental Section

Sample Preparation and Deposition. Keggin-type[45] HPAs with different heteroatoms, $H_nMW_{12}O_{40}$ (M = P, Si, B, Co), were investigated in this work. Commercially available $H_3PW_{12}O_{40}$ and $H_4SiW_{12}O_{40}$ samples were obtained from Aldrich Chemical Co. $H_5BW_{12}O_{40}$ and $H_6CoW_{12}O_{40}$ were prepared according to published methods.[46−52] Approximately 0.01 M aqueous solutions of each sample were prepared. A drop of solution was deposited on freshly cleaved HOPG and allowed to dry in air for ca. 45 min at room temperature for STM imaging. Pyridine exposure was carried out

(14) Chen, Q.; Perry, C. C.; Frederick, B. G.; Murray, P. W.; Haq, S.; Richardson, N. V. *Surf. Sci*. **2000**, *446*, 63.
(15) Silva, S. L.; Patel, A. A.; Pham, T. M.; Leibsle, F. M. *Surf. Sci*. **1999**, *441*, 351.
(16) Gimzewski, J. K.; Stoll, E.; Schlittler, R. R. *Surf. Sci*. **1987**, *181*, 267.
(17) Johansson, M. K.-J.; Gray, S. M.; Johansson, L. S. O. *J. Vac. Sci. Tehnol., B* **1996**, *14*, 1015.
(18) Valden, M.; Lai, X.; Goodman, D. W. *Science* **1998**, *281*, 1647.
(19) Bettac, A.; Koller, L.; Rank, V.; Meiwes-Broer, K. H. *Surf. Sci*. **1998**, *404*, 475.
(20) Kaba, M. S.; Song, I. K.; Barteau, M. A. *J. Phys. Chem*. **1996**, *100*, 19577.
(21) Kaba, M. S.; Song, I. K.; Barteau, M. A. *J. Vac. Sci. Technol., A* **1997**, *15*, 1299.
(22) Song, I. K.; Kaba, M. S.; Barteau, M. A.; Lee, W. Y. *Catal. Today* **1998**, *44*, 285.
(23) Kinne, M.; Barteau, M. A. *Surf. Sci*. **2000**, *447*, 105.
(24) Pope, M. T.; Müller, A. *Angew. Chem., Int. Ed. Engl*. **1991**, *30*, 34.
(25) *Polyoxometalates: from Platonic Solids to Anti-retroviral Activity*; Pope, M. T., Müller, A., Eds.; Kluwer Academic Publishers: Dordrecht, The Netherlands, 1994.
(26) *Chem. Rev*. **1998**, *98* (Special Thematic Issue on Polyoxometalates; Hill, C. L., Guest Ed.).
(27) Mori, H.; Mizuno, N.; Misono, M. *J. Catal*. **1990**, *131*, 133.
(28) Neumann, R. *Prog. Inorg. Chem*. **1998**, *47*, 317.
(29) Misono, M. *Catal. Rev.—Sci. Eng*. **1987**, *29*, 269.
(30) Kozhevnikov, I. V. *Catal. Rev.—Sci. Eng*. **1995**, *37*, 311.
(31) Hill, C. L.; Prosser-McCartha, C. M. *Coord. Chem. Rev*. **1995**, *143*, 407.
(32) Pope, M. T. *Heteropoly and Isopoly Oxometalates*; Springer-Verlag: New York, 1983.
(33) Keita, B.; Nadjo, L. *Surf. Sci.* **1991**, *254*, L443.
(34) Watson, B. A.; Barteau, M. A.; Haggerty, L.; Lenhoff, A. M.; Weber, R. S. *Langmuir* **1992**, *8*, 1145.
(35) Ge, M.; Zhong, B.; Klemperer, W. G.; Gewirth, A. A. *J. Am. Chem. Soc*. **1996**, *118*, 5812.
(36) Song, I. K.; Kaba, M. S.; Coulston, G.; Kourtakis, K.; Barteau, M. A. *Chem. Mater*. **1996**, *8*, 2352.
(37) Kaba, M. S.; Song, I. K.; Duncan, D. C.; Hill, C. L.; Barteau, M. A. *Inorg. Chem.* **1998**, *37*, 398.
(38) Song, I. K.; Kaba, M. S.; Barteau, M. A. *J. Phys. Chem*. **1996**, *100*, 17528.
(39) Kaba, M. S.; Barteau, M. A.; Lee, W. Y.; Song, I. K. *Appl. Catal., A* **2000**, *194*, 129.
(40) Müssig, H.-J.; Krüger, D.; Hinrich, S.; Hansson, P. O. *Surf. Sci*. **1994**, *314*, L884.
(41) Nosho, B. Z.; Weinberg, W. H.; Barvosa-Carter, W.; Bracker, A. S.; Mango, R.; Bennett, B. R.; Culbertson, J. C.; Shanabrook, B. V.; Whitman, L. J. *J. Vac. Sci. Technol., B* **1999**, *17*, 1786.
(42) Petukhov, A. G.; Demchenko, D. O.; Chantis, A. N. *J. Vac. Sci. Technol., B* **2000**, *18*, 2109.
(43) Kaba, M. S.; Song, I. K.; Barteau, M. A. *J. Phys. Chem*., in press.
(44) Okuhara, T.; Mizuno, N.; Misono, M. *Adv. Catal*. **1996**, *41*, 113.
(45) Keggin, J. F. *Nature* **1933**, *131*, 908.

by placing a drop of liquid pyridine on the previously deposited HPA layer and drying in air for ca. 1 h at room temperature. Reversibly adsorbed pyridine molecules were then removed by evacuating the sample at ca. 25 mTorr for 1 h at room temperature prior to the STM measurements.

Scanning Tunneling Microscopy and Tunneling Spectroscopy. STM images were obtained in air using a Topometrix TMX 2010 instrument. Mechanically formed Pt/Ir (90/10) tips were used as probes. Scanning was done in the constant-current mode at a positive sample bias of 100 mV and tunneling current of 1−2 nA. Tunneling spectra were measured in air. Both Topometrix TMX 2010 and LK Technologies LK-1000 STM instruments were used to confirm the consistency and reproducibility of tunneling spectra. All STM images presented in this paper are unfiltered, and the reported periodicities (lattice constants) represent average values determined by performing 2-dimensional fast Fourier transform (FFT) analyses on at least three images for each sample. Each image was acquired using a different tip; the tips were first calibrated by imaging bare HOPG to confirm the standard periodicity of HOPG (2.46 Å). Several tunneling spectra were then taken on the bare graphite section of the surface to ensure the stability of the tip and the reproducibility of the tunneling spectrum of HOPG. Once these had been established, the "good" tip would be moved to the HPA-covered section to image and obtain tunneling spectra of the HPA sample. To measure a tunneling spectrum, the sample bias was ramped from −2 to +2 V with respect to the tip, and the tunneling current was monitored. The voltage axis in the tunneling spectrum represents the potential applied to the sample relative to that of the tip.

Results and Discussion

Self-Assembled and Well-Ordered HPA Arrays. The size of Keggin-type[45] HPA is ca. 10−12 Å as determined by X-ray crystallography.[52,53] Figure 1 shows a polyhedral representation of the molecular structure of the pseudospherical (T_d symmetry) Keggin-type heteropolyanion $[PW_{12}O_{40}]^{3-}$.[32] The structure of $[PW_{12}O_{40}]^{3-}$ consists of a heteroatom, P, at the center of the anion cluster, tetrahedrally coordinated to four oxygen atoms. This tetrahedron is surrounded by 12 WO_6 octahedra. The van der Waals diameter along the 3-fold axis of symmetry (i.e., the vertical dimension of the structure in Figure 1) is 11.97 Å.[37,53] The primary structure, the Keggin structure,[45] of the heteropolyanion is relatively stable. In the solid state, the 3-dimensional arrangement of HPAs comprising heteropolyanions, protons, cations, water, and/or organics is called the secondary structure.[54] Protons in the bulk structure are highly solvated.[30] Unlike the relatively stable primary structure, the secondary structure is very labile and may change in different environments by either increasing or decreasing the interstitial space between heteropolyanions. Indeed Misono has suggested that HPAs in heterogeneous catalysis can function in some cases as a "pseudoliquid" phase.[29] Figure 2 shows the STM images of $H_nMW_{12}O_{40}$ (M = P, Si, B, Co) samples deposited on HOPG. All these STM images clearly show the formation of self-assembled and well-ordered HPA arrays on the graphite surface. The periodicities measured for 2-dimensional arrays and the included angles of the rhombohedral unit cells constructed from 2-dimensional FFT analysis are summarized in Table 1. The periodicities are 11−12 Å and are in good agreement with lattice constants obtained by STM[20−23,36−39] and X-ray crystallography.[32,52,53,55] All HPA samples examined in this work formed well-ordered arrays on graphite over scan areas of at least 200 Å by 200 Å. No

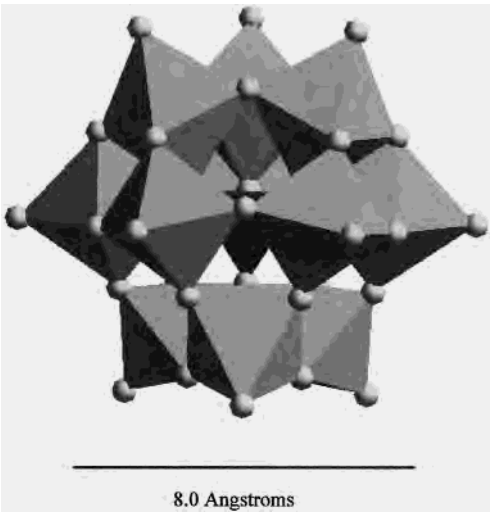

Figure 1. Polyhedral representation of the molecular structure of Keggin-type[45] heteropolyanion $[PW_{12}O_{40}]^{3-}$.

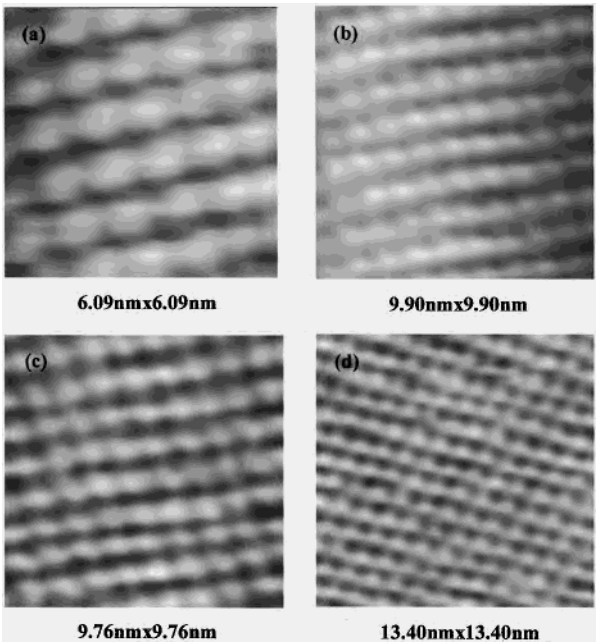

Figure 2. STM images of (a) $H_3PW_{12}O_{40}$, (b) $H_4SiW_{12}O_{40}$, (c) $H_5BW_{12}O_{40}$, and (d) $H_6CoW_{12}O_{40}$ freshly deposited on graphite.

(46) Rocchiccioli-Deltcheff, C.; Fournier, M.; Franck, R.; Thouvenot, R. *Inorg. Chem.* **1983**, *22*, 207.
(47) Rocchiccioli-Deltcheff, C.; Thouvenot, R.; Franck, R. *Spectrochim. Acta, A* **1976**, *32*, 587.
(48) Brown, D. H. *Spectrochim. Acta* **1963**, *19*, 583.
(49) Walmsley, F. *J. Chem. Educ.* **1992**, *69*, 936.
(50) Pope, M. T.; Varga, G. M., Jr. *Inorg. Chem.* **1966**, *5*, 1249.
(51) Hu, C.; Hashimoto, M.; Okuhara, T.; Misono, M. *J. Catal.* **1993**, *143*, 437.
(52) Nolan, A. L.; Allen, C. C.; Burns, R. C.; Craig, D. C.; Lawrance, G. A. *Aust. J. Chem.* **2000**, *53*, 59.
(53) Brown, G. M.; Noe-Spirlet, M. R.; Busing, W. R.; Levy, H. A. *Acta Crystallogr., B* **1977**, *33*, 1038.
(54) Misono, M. *Mater. Chem. Phys.* **1987**, *17*, 103.
(55) Hayashi, H.; Moffat, J. B. *J. Catal.* **1982**, *77*, 473.

Table 1. Lattice Constants and NDR Peak Voltages of $H_nMW_{12}O_{40}$ (M = P, Si, B, Co) Samples on a Graphite Surface

HPA sample	periodicity (Å)	included angle (deg)	NDR peak voltage (V)
$H_3PW_{12}O_{40}$	11.7 ± 0.3	79.5	-1.14 ± 0.09
$H_4SiW_{12}O_{40}$	11.2 ± 0.3	87.5	-1.19 ± 0.08
$H_5BW_{12}O_{40}$	11.4 ± 0.4	82.9	-1.28 ± 0.09
$H_6CoW_{12}O_{40}$	11.3 ± 0.3	73.2	-1.36 ± 0.09

systematic differences were observed in periodicities or included angles of HPA arrays with variations in heteroatom identity. The surface arrays of HPA samples were quite homogeneous. Small variations of periodicity for each HPA sample most likely do not arise from the inhomogeneity of the sample but from the STM imaging measurement, as the tip structure may change electronically during or between STM imaging and may drift slightly in a small scan area.

Our previous results[36] and those reported here suggest that the level of hydration of protons in HPA monolayers is much less than that in bulk 3-dimensional crystal structures for which compositions such as $H_3PW_{12}O_{40}\cdot 14H_2O$ and $H_3PW_{12}O_{40}\cdot 29H_2O$ have been reported.[56] In the case of monolayers of $[PMo_{12}O_{40}]^{3-}$, it was observed that the lattice constant increased by nearly 3 Å when protons were replaced by Cs^+, suggesting that the space occupied by protons was not consistent with the presence of large numbers of solvating water molecules. The lack of significant or systematic variation of lattice constants for the HPAs in Table 1 reinforces this conclusion. If the protons were highly solvated, one would expect that their resulting bulk would cause the lattice constants to increase progressively as the charge on the polyoxoanion (and therefore the number of counterions) increased. No such trend can be discerned for the series $H_3PW_{12}O_{40}$ through $H_6CoW_{12}O_{40}$ in Table 1. It should be noted that the similarity of lattice constants in Table 1 is not a consequence of strong interactions with, or periodicity imposed by, the underlying HOPG surface (hexagonal structure with 2.46 Å periodicity). We have previously reported a wide variety of lattice constants and packing motifs for monolayers of a large assortment of HPAs with Keggin, Dawson, and other framework structures;[20,36,37] none exhibit any discernible relationship to the HOPG surface structure.

NDR Behavior and Monolayer Array Verification. A typical tunneling spectrum taken at a position corresponding to the bright corrugations in the image of $H_4SiW_{12}O_{40}$ in Figure 2b is shown in Figure 3a. The spectrum shows a distinctive $I-V$ behavior at -1.2 V, referred to as NDR, because dI/dV is negative in this region. The NDR peak voltage was defined as the voltage at which the maximum current was observed in this region. Tunneling spectra taken at the interstitial spaces between bright corrugations in Figure 2b showed the typical $I-V$ response of graphite, indicating that the 2-dimensional array of $H_4SiW_{12}O_{40}$ on graphite is a monolayer at least in this region imaged, as previously demonstrated.[20−23,36−39] In some regions presumed to be multilayers, STM imaging was not attainable due to difficulties in electron tunneling through the insulating HPA multilayers. The NDR measurements themselves were carried out several times with at least three different tips to obtain more accurate and reproducible results, and to provide a basis for statistical analyses. The voltage resolution of $I-V$ spectra was 0.05 V. Figure 3b shows the distribution of NDR peak voltages for the $H_4SiW_{12}O_{40}$ sample. The NDR peak voltage of $H_4SiW_{12}O_{40}$ was found to be -1.19 ± 0.08 V. The NDR peak voltages of $H_nMW_{12}O_{40}$ (M = P, Si, B, Co) samples are listed in Table 1.

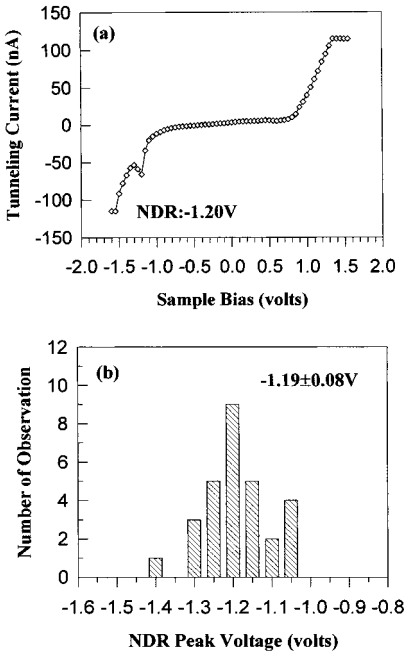

Figure 3. (a) Tunneling spectrum taken at $H_4SiW_{12}O_{40}$ corrugations (bright features) in Figure 2b. (b) Distribution of NDR peak voltages of $H_4SiW_{12}O_{40}$ arrays.

Correlation between NDR Peak Voltage and Reduction Potential. We have previously explained NDR in tunneling spectra of HPAs in terms of resonant tunneling through a double-barrier structure, with the HPA molecule acting as a quantum well.[20] A similar explanation for NDR observed for an Anderson-type $[PtMo_6O_{24}]^{4-}$ polyanion was also recently offered.[57] The STM images in this work were obtained at positive sample biases with respect to the tip. This means that electrons flow from the tip to the sample in the imaging mode of operation. NDR behavior in the tunneling spectra of HPAs is observed at negative sample biases, i.e., when electrons tunnel from the sample to the tip. Previous quantum chemical studies[58,59] of Keggin ions have suggested that the HOMO (highest occupied molecular orbital) consisting primarily of nonbonding p-orbitals on the terminal oxygens is little perturbed by framework substitutions in these structures. The LUMO (lowest unoccupied molecular orbital) consisting of an antibonding combination of d-orbitals on the metal centers and p-orbitals on the bridging oxygens is more sensitive to the framework

(56) Izumi, Y.; Urabe, K.; Onaka, M. *Zeolite, Clay, and Heteropoly Acid in Organic Reactions*; Kodansha: Tokyo, 1992.
(57) Dykhne, A. M.; Vasil'ev, S. Y.; Petrii, O. A.; Rudavets, A. G.; Tsirlina, G. A. *Dokl. Akad. Nauk* **1999**, *368*, 467.
(58) Taketa, H.; Katsuki, S.; Eguchi, K.; Seiyama, T.; Yamazoe, N. *J. Phys. Chem*. **1986**, *90*, 2959.
(59) Weber, R. S. *J. Phys. Chem*. **1994**, *98*, 2999.

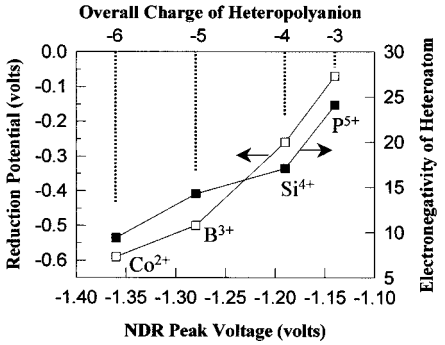

Figure 4. Correlation between the NDR peak voltage and heteroatom electronegativity[62] and between the NDR voltage and reduction potential[63,64] of $H_nMW_{12}O_{40}$ (M = P, Si, B, Co) HPAs.

composition. Thus, we suggest that NDR arises in these systems for electron tunneling from the graphite substrate to the metal tip mediated by the LUMO of the individual HPAs. We have previously demonstrated that the striking NDR behavior of nanostructured HPA arrays measured by STM is closely related to the electronic properties of these materials, and may serve as a correlating parameter for their redox properties.[20−23] The characteristic NDR peaks appeared at less negative applied voltages when the protons of the HPA were replaced by higher charged (more electronegative) cations such as Cu^{2+}; the NDR peaks shifted to higher negative voltages when the protons were replaced by lower charged (less electronegative) cations such as Cs^+. It has been suggested that copper, which has a higher electrostatic parameter than cesium, acts as a large electron reservoir to facilitate electron transfer to the heteropolyanion framework in reducing environments by providing a route for electron delocalization.[60] Countercation charge is only part of the story, however. Within families of HPA salts containing cations of the same valence, e.g., H^+ and Cs^+ and Ba^{2+}, Zn^{2+}, Co^{2+}, and Cu^{2+}, both the reduction potential and NDR peak position can vary substantially, as previously demonstrated.[20,61] For these countercation-exchanged systems, we have found the Tanaka electronegativity scale,[62] which includes charge, to be a useful correlating parameter. The HPAs containing more highly charged and more electronegative countercations were characterized by higher reduction potentials and showed NDR behavior at less negative applied voltages.[20−22]

Figure 4 shows the correlation between the NDR peak voltage and heteroatom electronegativity[62] and between the NDR voltage and reduction potential[63,64] of $H_nMW_{12}O_{40}$ (M = P, Si, B, Co) samples. Within this series, of course, each HPA is characterized by a different charge on the heteroatom, as also shown in Figure 4. Thus, one cannot comment on the variations with substitution of heteroatoms of like charge. However, for generality and for consistency of comparison with our previous studies[20−23,61] of countercation-exchanged HPAs, we have referenced the Tanaka electronegativity as a correlating parameter. This electronegativity scale takes into account both electron-donating and -accepting ability.[62] The Tanaka electronegativity was defined as $(1 + 2Z)X_o$, reflecting both charge (Z) and Pauling electronegativity (X_o). Reduction potentials of $H_nMW_{12}O_{40}$ (M = P, Si, B, Co) were taken from the literature.[63,64] NDR peak voltages of $H_nMW_{12}O_{40}$ (M = P, Si, B, Co) arrays appeared at less negative values with increasing reduction potential of the HPAs and with increasing charge or electronegativity of the heteroatom. Thus, the NDR peak voltages shifted to more negative values as the overall negative charge of the heteropolyanion increased. Clearly, these results reinforce the general conclusion that more reducible HPAs show NDR behavior at less negative applied voltages in their tunneling spectra. Interestingly and surprisingly, the NDR voltage appears at a less negative voltage, and the reduction potential increases, with increasing heteroatom electronegativity and charge within the series $H_nMW_{12}O_{40}$ (M = P, Si, B, Co), as observed for cation-exchanged HPAs.[20−23,61] These NDR voltage and reduction potential dependencies track the charge on the polyanion unit of the HPA, as seen in other studies.[20,50,63,65,66] Recent electrochemical, spectroscopic. and kinetic studies clarify some thermodynamic and kinetic aspects of the role of the HPA charge (and its modification by ion-pairing) on the HPA reduction potential and reactivity.[65,66] Within families of 1:1 HPA ion pairs $[(Q^+)(X^{n+}VW_{11}O_{40})]^{(8-n)-}$ (Q = Li, Na, K; X = P, Si, Al), for example, it has been demonstrated that reduction potentials increased with increasing heteroatom charge, and with increasing countercation size (with the decrease in size of the solvated ion pair).[65]

Pyridine Interaction with HPA Arrays. A 3-dimensional crystal structure of the pyridinium salt of $PW_{12}O_{40}^{3-}$ has been reported.[67] In the 3-dimensional structure, it was concluded that the pyridine molecules were paired around H^+, forming $(C_5H_5N)H^+(NC_5H_5)$ cations. This structural motif involving protonated solvent dimers as counterions to the polyanion units is well established by X-ray diffraction spectroscopic and reactivity studies.[68−70] Figure 5 shows the 2-dimensional STM images of $H_nMW_{12}O_{40}$ (M = P, Si, B, Co) samples deposited on HOPG, after pyridine exposure. It is reasonable to assume that any water molecules present initially are removed by the sequence of exposure to liquid pyridine, drying, and evacuation. All STM images in Figure 5 clearly show the formation of self-assembled and well-ordered HPA arrays on the graphite surface. The periodicities measured for 2-dimensional arrays and included angles of the unit cells constructed on the basis of lattice constants determined from 2-dimensional FFT are summarized in Table 2. Unlike the fresh HPA sample arrays shown in Figure 2, pyridine-

(60) Kim, H. C.; Moon, S. H.; Lee, W. Y. *Catal. Lett.* **1991**, 447.
(61) Song, I. K.; Barteau, M. A. *J. Mol. Catal., A,* in press.
(62) Tanaka, K.; Ozami, A. *J. Catal.* **1967**, *8*, 1.
(63) Alternau, J. J.; Pope, M. T.; Prados, R. A.; So, H. *Inorg. Chem.* **1975**, *14*, 417.
(64) Sadakane, M.; Steckhan, E. *Chem. Rev.* **1998**, *98*, 219.
(65) Grigoriev, V. A.; Hill, C. L.; Weinstock, I. A. *J. Am. Chem. Soc.* **2000**, *122*, 3544.
(66) Grigoriev, V. A.; Cheng, D.; Hill, C. L.; Weinstock, I. A. *J. Am. Chem. Soc.* **2001**, *123*, 5292.
(67) Hashimoto, M.; Misono, M. *Acta Crystallogr., C* **1994**, *50*, 231.
(68) Prosser-McCartha, C. M.; Kadkhodayan, M.; Williamson, M. M.; Bouchard, D. A.; Hill, C. L. *J. Chem. Soc., Chem. Commun.* **1986**, 1747.
(69) Hill, C. L.; Bouchard, D. A.; Kadkhodayan, M.; Williamson, M. M.; Schmidt, J. A.; Hilinski, E. F. *J. Am. Chem. Soc.* **1988**, *110*, 5471.
(70) Le Maguerès, P.; Hubig, S. M.; Lindeman, S. V.; Veya, P.; Kochi, J. K. *J. Am. Chem. Soc.* **2000**, *122*, 10073.

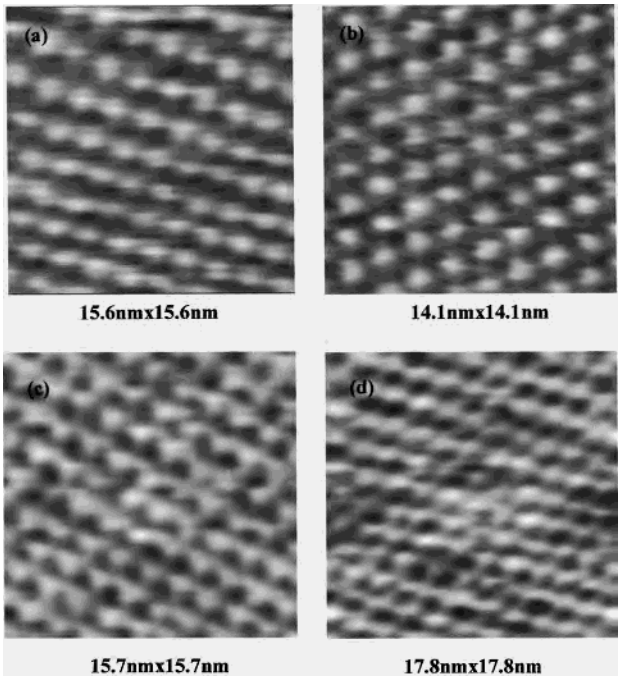

Figure 5. STM images of (a) $H_3PW_{12}O_{40}$, (b) $H_4SiW_{12}O_{40}$, (c) $H_5BW_{12}O_{40}$, and (d) $H_6CoW_{12}O_{40}$ on graphite after pyridine exposure.

Table 2. Lattice Constants and NDR Peak Voltages of $H_nMW_{12}O_{40}$ (M = P, Si, B, Co) Samples on a Graphite Surface after Pyridine Exposure

HPA sample	periodicity (Å)	included angle (deg)	NDR peak voltage (V)
$H_3PW_{12}O_{40}$	18.2 ± 0.4	59.1	-0.66 ± 0.05
$H_4SiW_{12}O_{40}$	17.5 ± 0.6	66.6	-0.85 ± 0.07
$H_5BW_{12}O_{40}$	17.4 ± 0.5	73.2	-1.01 ± 0.08
$H_6CoW_{12}O_{40}$	17.5 ± 0.5	58.5	-1.12 ± 0.09

exposed HPA samples form roughly hexagonal arrays. Moreover, the periodicities of pyridine-exposed HPA arrays increased by ca. 6 Å, roughly the molecular size of pyridine, compared to those of fresh samples. These results demonstrate that pyridine molecules are bound at the acid sites in the interstitial space between heteropolyanions in the 2-dimensional surface arrays, in a manner similar to the bonding in 3-dimensional solids. These results also indicate that 2-dimensional HPA arrays were rearranged and expanded upon pyridine exposure. However, as in previous STM images of HPAs,[38] the pyridinium ions, like other charge-compensating cations in these arrays, were not imaged directly.

The interaction of pyridine with HPA arrays was also confirmed by tunneling spectroscopy measurements. A typical tunneling spectrum taken at the bright corrugations of pyridine-exposed $H_4SiW_{12}O_{40}$ imaged in Figure 5b is shown in Figure 6a, and the distribution of NDR peak voltages for the pyridine-exposed $H_4SiW_{12}O_{40}$ sample is shown in Figure 6b. The NDR peak voltage of the pyridine-exposed $H_4SiW_{12}O_{40}$ sample was found to be -0.85 ± 0.07 V. Introduction of electron-rich pyridine molecules into $H_4SiW_{12}O_{40}$ arrays leads to an NDR voltage shift of 0.34 V, from -1.19 to -0.85 V. The NDR peak voltages of pyridine-exposed $H_nMW_{12}O_{40}$ (M = P, Si, B, Co) samples are listed in Table 2. The shift of NDR peak voltages of HPA samples to less negative applied voltages after pyridine adsorption

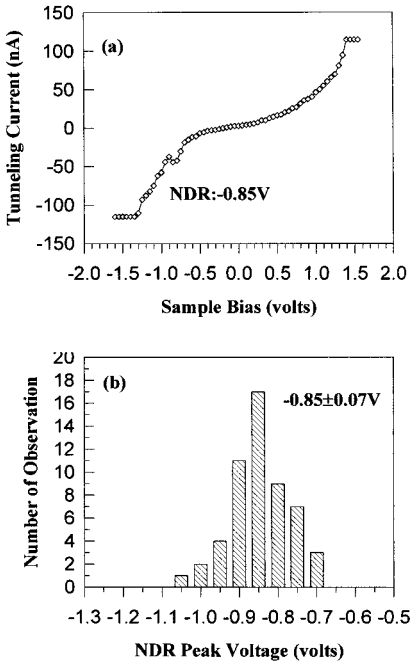

Figure 6. (a) Tunneling spectrum taken at bright features in the pyridine-exposed $H_4SiW_{12}O_{40}$ array in Figure 5b. (b) Distribution of NDR peak voltages of pyridine-exposed $H_4SiW_{12}O_{40}$ arrays.

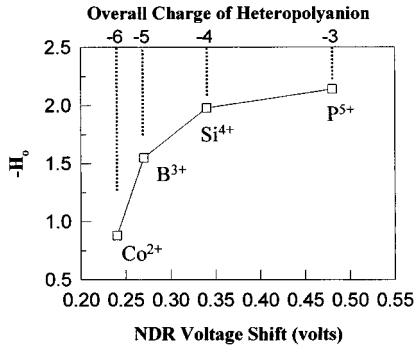

Figure 7. Correlation between the acid strengths[51,71] of $H_nMW_{12}O_{40}$ (M = P, Si, B, Co) HPAs and their NDR voltage changes after pyridine exposure.

was attributed to the replacement of protons with pyridinium ions.[39] This effect on the NDR position is comparable to that obtained by exchanging more highly charged or more electronegative countercations for protons.[20,38] Because the introduction of large pyridinium ions also increases the separation between heteropolyanions as noted, the interactions between the anions may also be altered. However, the extent to which changes in electrostatic interactions may contribute to NDR peak shifts is unclear at present.

Correlation between NDR Peak Shift and Acid Strength. We have shown that NDR peak voltages of HPA samples with different heteroatoms were strongly affected by the pyridine binding to the acid sites of the HPAs. We consider below whether the magnitudes of the NDR peak shifts of different HPAs measured before and after pyridine adsorption may serve as an indicator of their acid properties. It can be inferred that the strong interaction of base molecules with acid sites of HPA arrays may give rise to large NDR shifts. Figure 7 shows the correlation between NDR voltage shifts for as-deposited versus pyridine-exposed HPA arrays, de-

termined from the data in Tables 1 and 2, and the acid strengths of $H_nMW_{12}O_{40}$ (M = P, Si, B, Co) samples reported in the literature.[51,71] It is noteworthy that the acid strength of $H_nMW_{12}O_{40}$ (M = P, Si, B, Co) samples can be directly correlated with NDR peak voltage shifts upon pyridine exposure. $H_3PW_{12}O_{40}$, which has the highest acid strength among this series of heteroatom-substituted HPAs, experiences the largest NDR peak shift upon pyridine exposure. This implies that the change in the electronic environment of the heteropolyanion upon proton transfer to pyridine is greatest for the strongest proton donor, as expected. The same trend has been observed for framework-metal-cation-substituted HPAs. $H_3PW_{12}O_{40}$, which has the highest acid strength in the series $H_3PMo_{12-x}W_xO_{40}$ ($x = 0-12$), exhibited the largest NDR peak shift upon pyridine exposure.[39] Thus, we conclude that NDR voltage shifts of HPA monolayers measured by STM can be used to track their acid properties.

Conclusions

Nanoscale characterization of acid and redox properties of Keggin-type HPAs containing different heteroatoms, $H_nMW_{12}O_{40}$ (M = P, Si, B, Co), was carried out by STM and TS. HPA samples were deposited on HOPG surfaces to obtain images and tunneling spectra by STM before and after pyridine adsorption. All HPA samples formed self-assembled and well-ordered 2-dimensional arrays on graphite before and after pyridine adsorption. NDR peak voltages of fresh HPA samples were well correlated with the reduction potentials of the HPAs. NDR peak voltages of HPA samples appeared at less negative voltages with increasing reduction potential of the HPAs, and with increasing charge and electronegativity of the heteroatom, i.e., with decreasing overall negative charge of the heteropolyanion. Introduction of pyridinium cations into the HPA arrays resulted in expansion of the arrays and shifts of their NDR peak voltages to less negative values. The NDR shift of HPAs obtained before and after pyridine adsorption was correlated with the acid strengths of $H_nMW_{12}O_{40}$ (M = P, Si, B, Co) samples. It was confirmed that $H_3PW_{12}O_{40}$, the member of this series having the highest acid strength, experienced the largest NDR peak shift upon pyridine adsorption. Thus, the NDR shift measured on the nanostructured HPA arrays with STM may serve as a probe of the acid properties of bulk HPAs.

Acknowledgment. The Topometrix TMX 2010 was acquired via an equipment grant from the U.S. Department of Energy. I.K.S. acknowledges fellowship support from the Seoam Scholarship Foundation. The work at Emory University was funded by the National Science Foundation (Grant No. CHE-9975453).

IC010832D

(71) Okuhara, T.; Hu, C.; Hashimoto, M.; Misono, M. *Bull. Chem. Soc. Jpn.* **1994**, *67*, 1186.